THE JOURNAL OF BIOLOGICAL CHEMISTRY
Vol. 277, No. 28, Issue of July 12, pp. 25106–25114, 2002

*Printed in U.S.A.*

# Inhibition of *Plasmodium falciparum* Triose-phosphate Isomerase by Chemical Modification of an Interface Cysteine

ELECTROSPRAY IONIZATION MASS SPECTROMETRIC ANALYSIS OF DIFFERENTIAL CYSTEINE REACTIVITIES*

Received for publication, March 13, 2002, and in revised form, May 1, 2002
Published, JBC Papers in Press, May 2, 2002, DOI 10.1074/jbc.M202419200

**Kapil Maithal‡§, Gudihal Ravindra‡, Hemalatha Balaram¶, and Padmanabhan Balaram‡‖**

*From the ‡Molecular Biophysics Unit, Indian Institute of Science, Bangalore 560012, and the ¶Molecular Biology and Genetics Unit, Jawaharlal Nehru Center for Advanced Scientific Research, Jakkur Campus, Jakkur P. O., Bangalore 560004, India*

***Plasmodium falciparum* triose-phosphate isomerase, a homodimeric enzyme, contains four cysteine residues at positions 13, 126, 196, and 217 per subunit. Among these, Cys-13 is present at the dimer interface and is replaced by methionine in the corresponding human enzyme. We have investigated the effect of sulfhydryl labeling on the parasite enzyme, with a view toward developing selective covalent inhibitors by targeting the interface cysteine residue. Differential labeling of the cysteine residues by iodoacetic acid and iodoacetamide has been followed by electrospray ionization mass spectrometry and positions of the labels determined by analysis of tryptic fragments. The rates of labeling follows the order Cys-196 > Cys-13 ≫ Cys-217/Cys-126, which correlates well with surface accessibility calculations based on the enzyme crystal structure. Iodoacetic acid labeling leads to a soluble, largely inactive enzyme, whereas IAM labeling leads to precipitation. Carboxyl methylation of Cys-13 results in formation of monomeric species detectable by gel filtration. Studies with an engineered C13D mutant permitted elucidation of the effects of introducing a negative charge at the interface. The C13D mutant exhibits a reduced stability to denaturants and 7-fold reduction in the enzymatic activity even under the concentrations in which dimeric species are observed.**

The search for new therapeutic agents active against various pathogens has led to the development of inhibitors targeted to inactivate key parasitic enzymes (1–6). These approaches have led to targeting the enzymes present typically in the pathogen only (7) or selectively targeting the pathogen enzyme, if the homologous form exists in the host (8). Two distinct approaches to inactivate target enzymes may be considered. First, the design of inhibitors that compete for the active site, and second, the design of molecules that target subunit interfaces in multimeric proteins and interfere with protein assembly. In the case of many key enzymes the high degree of conservation of the active site in both host and parasite enzymes renders selective targeting difficult. Interfaces may show greater structural variations permitting a distinction between the host and the pathogen enzymes. Two distinct strategies usually considered for disrupting intersubunit contacts in proteins are: (i) the design of synthetic peptides and peptidomimetics of interface segments, which may interfere with the subunit association (9–11), and (ii) covalent chemical modification of reactive residues at the interface, which may cause disruption of the oligomeric state of the protein (12–14). In this regard, glycolytic enzymes are attractive targets, primarily because of their central role in energy production in the parasites (15–18).

Triose-phosphate isomerase (TIM)[1] is an important glycolytic enzyme that catalyzes the interconversion of glyceraldehyde 3-phosphate to dihydroxyacetone phosphate (19, 20). From the available knowledge of the structure of TIMs it is seen that the enzyme is a homodimeric protein, except in *Thermotoga maritima* and *Pyrococcus woesei*, where it is found to be tetrameric (21, 22). Each monomer exhibits a pseudo-8-fold symmetry with a central core made up of eight $\beta$-strands surrounded by eight $\alpha$-helices, which are linked together by loops (23). The enzyme has been found to be fully active only as a dimer, but there is no evidence for cooperativity (24). The dissociation constant of the dimeric trypanosomal TIM has been reported as $10^{-11}$ M$^{-1}$ (25). These studies reveal that the dimer is quite stable and is the active form of the protein. In fact, there are several reports that suggest that mutations at the subunit interface of the protein destabilize the dimer (26–32) leading to either complete inactivation or drastic decrease in the activity of the enzyme (25, 33). This knowledge has led to a renewed interest in this enzyme because it could serve as a drug target in many parasitic protozoans.

In the case of TIMs from parasites such as *Trypanosoma brucei* (34), *Trypanosoma cruzi* (35), *Plasmodium falciparum* (36), and *Leishmania mexicana* (37), a cysteine residue is present at the dimer interface; interestingly, in the enzyme from mammals the corresponding residue is methionine, whereas in yeast it is leucine (Fig. 1). Recent studies on trypanosomal and leishmanial TIMs reveal that derivatization of an interface cysteine residue using sulfhydryl reagents such as methyl methanethiosulfonate and 5,5′-dithiobis(2-nitrobenzoic acid) induces progressive structural alterations and abolition of the

* This work was supported in part by a grant from the Department of Science and Technology, Government of India. The mass spectrometry facility is supported by the Drug and Molecular Design program of the Department of Biotechnology, Government of India. The costs of publication of this article were defrayed in part by the payment of page charges. This article must therefore be hereby marked "*advertisement*" in accordance with 18 U.S.C. Section 1734 solely to indicate this fact.

§ Recipient of a research associateship from Department of Biotechnology, Government of India.

‖ To whom correspondence should be addressed. Tel.: 91-80-309-2337; Fax: 91-80-334-1683 or 91-80-334-8535; E-mail: pb@mbu.iisc.ernet.in.

[1] The abbreviations used are: TIM, triose-phosphate isomerase; $C_m$, concentration of urea at which 50% of the protein is unfolded; ESI-MS, electrospray ionization mass spectrometry; HPLC, high performance liquid chromatography; IAA, iodoacetic acid; IAM, iodoacetamide; LC, liquid chromatography; PfTIM, *P. falciparum* triose-phosphate isomerase; TIMWT, wild type TIM.

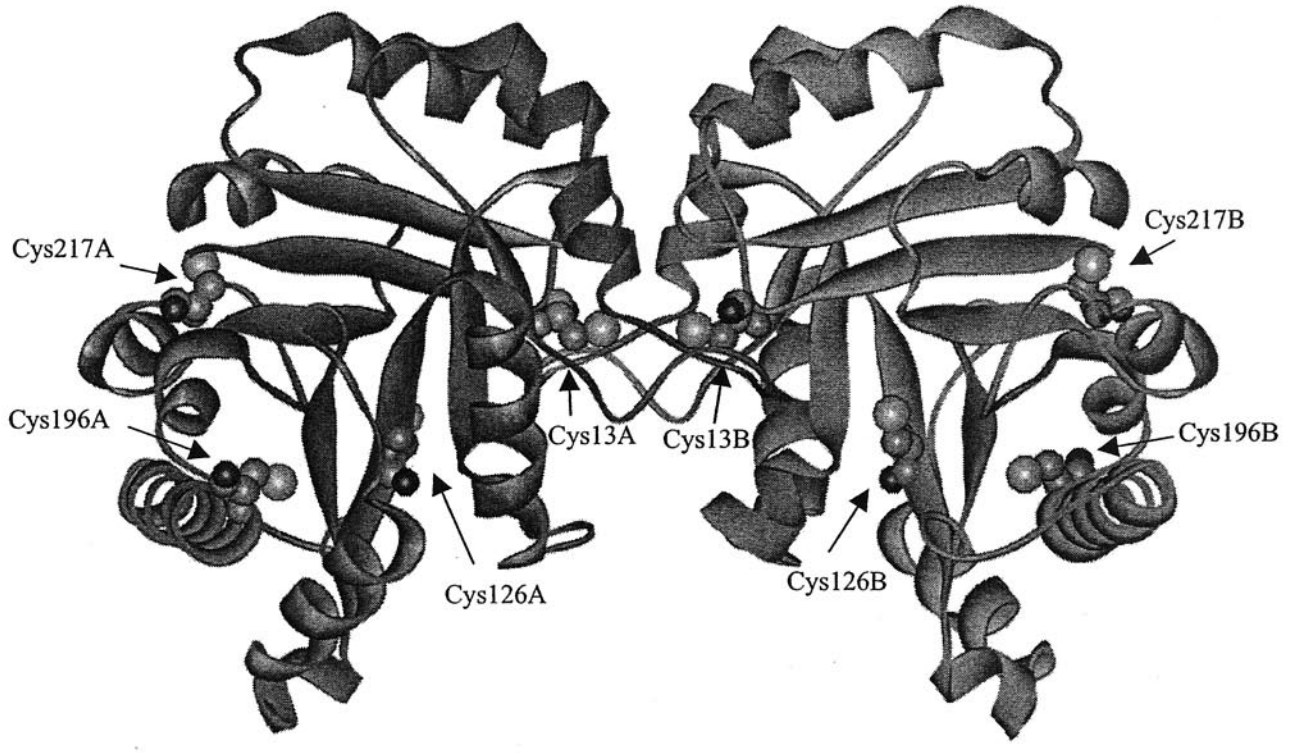


```
                                    13
TPIS_TRYBB      -MSKPQPIAAANWKCNGSQQSLSELIDLFNSTSIN-HDVQCVVASTFVHLAMTKERLSHPKFV
TPIS_TRYCR      MASKPQPIAAANWKCNGSESLLVPLIETLNAATFD-HDVQCVVAPTFLHIPMTKARLTNPKFQ
TPIS_LEIME      MSAKPQPIAAANWKCNGTTASIEKLVQVFNEHTIS-HDVQCVVAPTFVHIPLVQAKLRNPKYV
TPIS_HUMAN      -APSRKFFVGGNWKMNGRKQSLGELIGTLNAAKVP-ADTEVVCAPPTAYIDFARQKLD-PKIA
TPIS_RABIT      -APSRKFFVGGNWKMNGRKKNLGELITTLNAAKVP-ADTEVVCAPPTAYIDFARQKLD-PKIA
TPIS_YEAST      ---ARTFFVGGNFKLNGSKQSIKEIVERLNTASIP-ENVEVVICPPATYLDYSVSLVKKPQVT
TPIS_PLAFA      --MARKYFVAANWKCNGTLESIKSLTNSFNNLDFDPSKLDVVVFPVSVHYDHTRKLLQ-SKFS

TPIS_TRYBB      IAAQNAIAKS-GAFTGEVSLPILKDFGVNWIVLGHSERRAYYGETNEIVADKVAAAVASGFMV
TPIS_TRYCR      IAAQNAITRS-GAFTGEVSLQILKDYGISWVVLGHSERRLYYGETNEIVAEKVAQACAAGFHV
TPIS_LEIME      ISAENAIAKS-GAFTGEVSMPILKDIGVHWVILGHSERRTYYGETDEIVAQKVSEACKQGFMV
TPIS_HUMAN      VAAQNCYKVTNGAFTGEISPGMIKDCGATWVVLGHSERRHVFGESDELIGQKVAHALAEGLGV
TPIS_RABIT      VAAQNCYKVTNGAFTGEISPGMIKDCGATWVVLGHSERRHVFGESDELIGQKVAHALSEGLGV
TPIS_YEAST      VGAQNAYLKASGAFTGENSVDQIKDVGAKWVILGHSERRSYFHEDDKFIADKTKFALGQGVGV
TPIS_PLAFA      TGIQNVSKFGNGSYTGEVSAEIAKDLNIEYVIIGHFERRKYFHETDEDVREKLQASLKNNLKA
                   126
TPIS_TRYBB      IACIGETLQERESGRTAVVVLTQIAAIAKKLKKADWAKVVIAYEPVWAIGTGKVATPQQAQEA
TPIS_TRYCR      IVCVGETNEEREAGRTAAVVLTQLAAVAQKLSKEAWSRVVIAYEPVWAIGTGKVATPQQAQEV
TPIS_LEIME      IACIGETLQQREANQTAKVVLSQTSAIAAKLTKDAWNQVVLAYEPVWAIGTGKVATPEQAQEV
TPIS_HUMAN      IACIGEKLDEREAGITEKVVFEQTKVIADNVK--DWSKVVLAYEPVWAIGTGKTATPQQAQEV
TPIS_RABIT      IACIGEKLDEREAGITEKVVFEQTKVIADNVK--DWSKVVLAYEPVWAIGTGKTATPQQAQEV
TPIS_YEAST      ILCIGETLEEKKAGKTLDVVERQLNAVLEEVK--DWTNVVVAYEPVWAIGTGLAATPEDAQDI
TPIS_PLAFA      VVCFGESLEQREQNKTIEVITKQVKAFVDLID--NFDNVILAYEPLWAIGTGKTATPEQAQLV
                          196                                   217
TPIS_TRYBB      HALIRSWVSSKIGADVAGELRILYGGSVNGKNARTLYQQRDVNGFLVGGASLKPEFVDIIKATQ
TPIS_TRYCR      HELLRRWVRSKLGTDIAAQLRILYGGSVTAKNARTLYQMRDINGFLVGGASLKPEFVEIIEATK
TPIS_LEIME      HLLLRKWVSENIGTDVAAKLRILYGGSVNAANAATLYAKPDINGFLVGGASLKPEFRDIIDATR
TPIS_HUMAN      HEKLRGWLKSNVSDAVAQSTRIIYGGSVTGATCKELASQPDVDGFLVGGASLKPEFVDIINAKQ
TPIS_RABIT      HEKLRGWLKSNVSDAVAQSTRIIYGGSVTGATCKELASQPDVDGFLVGGASLKPEFVDIINAKQ
TPIS_YEAST      HASIRKFLASKLGDKAASELRILYGGSANGSNAVTFKDKADVDGFLVGGASLKPEFVDIINSRN
TPIS_PLAFA      HKEIRKIVKDTCGEKQANQIRILYGGSVNTENCSSLIQQEDIDGFLVGNASLKESFVDIIKSAM
```

FIG. 1. **Placement of cysteine residues in PfTIM and comparison of similar positions in some other species.** *Top*, three-dimensional view of the crystal structure of PfTIM showing the positions of cysteine residues (PDB code 1ydv). *Bottom*, sequence alignment of TIMs from some species, *highlighting* the amino acid residues in other species at positions corresponding to cysteine in PfTIM.

catalytic activity (12, 15, 35, 38, 39). Although these studies have revealed quite clearly that the interface cysteine residue is critical for the enzymatic activity, a clear correlation of the rates of cysteine labeling with enzyme inactivation and structural perturbation is not available. The interfacing of electrospray ionization mass spectrometry (ESI-MS) with protein chemistry allows convenient monitoring of the rates of covalent chemical modification. We have earlier described the structural characteristics of *P. falciparum* TIM (PfTIM) which also contains an interface cysteine residue, Cys-13 (29, 30, 36). In addition, PfTIM has three more cysteine residues at positions 126, 196, and 217 (Fig. 1). In this report we probe the differential reactivity of these four cysteine residues with sulfhydryl-modifying reagents iodoacetic acid (IAA) and iodoacetamide (IAM) using ESI-MS. We demonstrate that labeling of the interface cysteine residue Cys-13 results in weakening of the intersubunit interactions, leading to dimer dissociation with concomitant loss of enzymatic activity. To examine the effect of introducing a negative charge at the interface, as is the case in carboxyl methylated Cys-13, we have examined the stability and activity of a site-directed mutant, C13D.

TABLE I
*Surface accessibility of cysteine residues in P. falciparum triose-phosphate isomerase*

| Cysteine residue no. | Surface accessibility[a] | |
|---|---|---|
| | Monomer | Dimer |
| | % | |
| 13A (B) | 90.2 (90.1) | 0.1 (0) |
| 126A (B) | 0 (0) | 0 (0) |
| 196A (B) | 36.5 (21.2) | 36.5 (21.1) |
| 217A (B) | 2.8 (4.4) | 2.8 (4.4) |

[a] Surface accessibility calculations done using a probe radius of 1.4 Å water molecule, van der Waals radii of all of the heavy atoms in the protein were taken from, Chothia (46). The program used was NACCESS version 2.1. 100% was taken as the accessibility of the cysteine residue in a model, Gly-Cys-Gly in an extended conformation.

## EXPERIMENTAL PROCEDURES

*Materials*—The PfTIM gene was cloned and expressed in *Escherichia coli* as described before by Ranie *et al*. (40). IAA, IAM, 5,5′-dithiobis(2-nitrobenzoic acid), α-glycerolphosphate dehydrogenase, NADH, and glyceraldehyde-3-phosphate dehydrogenase were purchased from Sigma and used without further purification. The substrate glyceraldehyde 3-phosphate was obtained as a diethylacetal monobarium salt and processed to its active form according to manufacturer's instructions. The concentration of glyceraldehyde 3-phosphate extracted was estimated using glyceraldehyde-3-phosphate dehydrogenase. Absorbance spectra were recorded on a double beam spectrophotometer (Shimadzu UV210A) using 1-cm path length quartz cuvettes. Restriction enzymes and T4 DNA ligase were procured from Amersham Biosciences. *Taq* DNA polymerase was from Bangalore Genei Private Ltd., Bangalore, India. Conditions recommended by the manufacturer were used for all molecular biology reagents. The *E. coli* strain AA200 was a gift from Dr. Barbara Bachmann of the *E. coli* Genetic Stock Centre, New Haven, CT.

*Mutagenesis*—A plasmid, pTIMC1, carrying wild type PfTIM in the *E. coli* expression vector pTRC99A (40), was used for the construction of

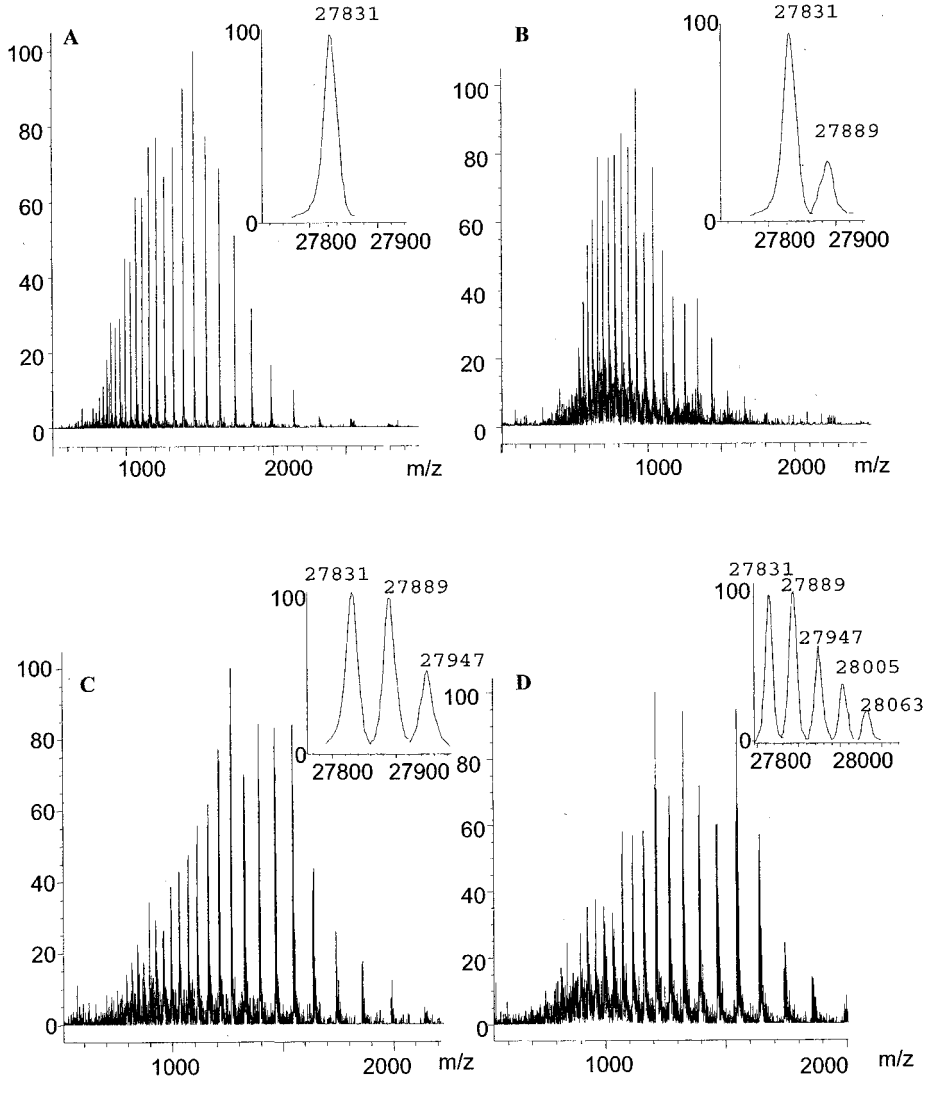


FIG. 2. **Mass spectral analysis of the IAA labeling reaction.** The ESI-MS of differentially labeled PfTIM after the reaction was initiated with IAA is shown. *A*, unlabeled protein; *B–D*, at different time intervals after initiation of the reaction; *B*, 60 min; *C*, 150 min; and *D*, 240 min. The *insets* show the derived masses.

the mutant, C13D. The mutation was introduced by PCR, and the oligonucleotides used were C13D (5′-CCACATGGCTAGAAAATATTT-TGTCGCAGCAAACTGGAAA**GA**AATGGAACT-3′, highlighted letters indicate site of mutation) and TIM8 (5′-ACGGATCCTTACATAG-CACTTTTTATTATATC-3′). PCR was carried out, for 30 cycles, in a 50-$\mu$l solution containing 10 mM Tris-HCl, pH 9.0, 1.5 mM $MgCl_2$, 50 mM KCl, 0.01% gelatin, 2.5 mM dNTPs, 400 nM oligonucleotide primers, 5 ng of template, and 2 units of *Taq* DNA polymerase with denaturation at 93 °C for 15 s, annealing at 55 °C for 15 s, and extension at 73 °C for 30 s. The amplified product (700 bp) was purified on agarose gel, digested with restriction enzymes *Nco*I and *Bam*HI, and again purified using Geneclean II (BIO 101, Inc., Vista, CA). This DNA fragment was ligated with *Nco*I/*Bam*HI-restricted plasmid pTRC99A using T4 DNA ligase. The ligation mixture was used to transform the *E. coli* strain AA200 (*garB*10, *fhuA*22, *ompF*627, *fadL*701, *relA*1, *pit*-10, *spoT*1, *tpi*-1, *phoM*510, *merB*1). Colonies obtained were screened for the presence of the insert (750 bp). One of the positive clones, pTIMC13D1, was sequenced using an automated DNA sequencing system and confirmed to contain the mutation. PTIMC13D/AA200 induced with 1 mM isopropyl-1-thio-$\beta$-D-galactopyranoside was analyzed on SDS-PAGE and found to overexpress a protein of the expected size (28 kDa). On analysis of PfTIM C13D by mass spectrometry, a mass of 27,815 Da was obtained. This confirmed the presence of only the required mutation (Cys-13 → Asp) in the mutant C13D.

*Labeling*—The cysteine residues were labeled by incubating 1 mg of protein with 9.3 mg of the sulfhydryl reagent IAA or IAM in 600 mM Tris-HCl, pH 8.7, buffer for varying periods. Excess label was removed from the reaction mixture by chromatography on a Sephadex G-10 gel filtration column before mass spectral and biochemical studies.

*Enzymatic Activity*—Kinetic measurements were carried out according to the method of Plaut and Knowles (41) on a Shimadzu UV210A double beam spectrophotometer at room temperature. The cuvette contained 100 mM triethanolamine buffer, pH 7.6, 5 mM EDTA, 0.5 mM NADH, 20 $\mu$g/ml $\alpha$-glycerolphosphate dehydrogenase, and 1 mM glyceraldehyde 3-phosphate. The enzyme concentration was kept as 0.5 nM for the wild type enzyme and 1 $\mu$M for the C13D mutant. Enzyme activity was determined by monitoring the decrease in absorbance at 340 nm.

*Mass Spectrometry*—All LC-ESI-MS spectra were recorded on a Hewlett-Packard (model HP-1100) electrospray mass spectrometer coupled to an online 1100 series HPLC. A linear gradient of increasing percentage of acetonitrile was used as the mobile phase at a flow rate of 0.4 ml/min. A Zorbax SB-phenyl (4.6 mm × 25 cm) reverse phase column was used to separate the tryptic peptides. ESI was carried out using a capillary with an inner diameter of 0.1 mm. The tip was held at 5,000 V in a positive ion detection mode. Nebulization was assisted by $N_2$ gas (99.8%) at a flow rate of 10 liters/min. The spray chamber was held at 300 °C. The ion optics zone was optimized for maximal ion transmission. The best signal was obtained when a declustering potential (fragmentor voltage) of 200 V was set for detection. Data were acquired across a mass range of 125–3,000 *m/z* using a conventional quadrupole with a cycle time of 3 s. The spectrometer was tuned using five calibration standards provided by the manufacturer. Data processing was done using the deconvolution module of the Chemstation software to detect multiple charge states and obtain derived masses of the protein fragments.

*Fluorescence Spectroscopy*—Fluorescence emission spectra were recorded on a Hitachi 650–60 spectrofluorometer. The protein samples were excited at 280 nm and the emission spectra recorded from 300 to 400 nm. Excitation and emission band passes were kept as 5 nm. Corrections for inner filter effects were made to obtain the final spectra.

*Far UV-Circular Dichroism*—Far UV-CD measurements were carried out on a Jasco J-715 spectropolarimeter. Ellipticity changes at 220 nm were monitored to follow the unfolding transition. A path length of 1 mm was used, and the spectra were averaged over four scans at a scan speed of 10 nm/min.

*Gel Filtration*—Analytical gel filtration profiles for differentially labeled cysteines were done on a TSK 3000SW gel filtration column fitted to a Hewlett-Packard 1100 series HPLC. The column was calibrated with standard proteins. The protein was eluted at a flow rate of 0.4 ml/min with 100 mM Tris-HCl, pH 8.0, containing 150 mM NaCl.

## RESULTS AND DISCUSSION

The crystal structure of PfTIM, determined at 2.2 Å resolution, is a homodimer, with a very high structural similarity to all other known TIM structures (36). The interface is tightly packed and upon dimerization, 1,654 $Å^2$ of the total surface

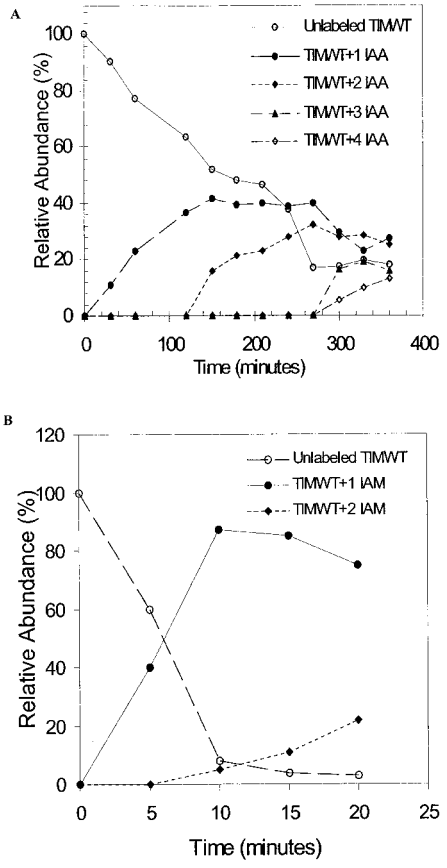


FIG. 3. **Abundance of differentially labeled species.** The relative abundance of IAA- and IAM-labeled species after the initiation of the labeling reaction is shown. The proportions of the differentially labeled species were estimated directly from the observed intensities in the deconvoluted mass spectrum assuming that all of the species ionize with equal efficiency. The error in determining relative abundance is about ±10%.

area per monomer is buried at the interface (36). Each of the subunits contains four cysteine residues (Fig. 1). Among them, Cys-13 is of special interest because it is absent in human TIM (see comparison of sequences in Fig. 1). Cys-13 is present on loop 1 at the interface and lies very close to the active site residues, Lys-12, His-95, and Glu-165. The thiol side chain points toward the interface loop region of the other subunit (Asn-71 to Ser-79) (the residue numbering used here follows the PfTIM sequence as reported earlier (36)). Indeed, Cys-13 has been used to engineer a pair of symmetric intersubunit disulfides in the mutant Y74C (30). The other three cysteine residues are at positions 126, 196, and 217. Cys-126 is located on $\beta$-strand 4, whereas Cys-196 and Cys-217 are found on helix 6 and helix 7, respectively, of the $\alpha_8/\beta_8$ TIM barrel (36). Among the four cysteines it is observed that Cys-126 is conserved in all known TIMs and is completely buried. Table I summarizes the results of surface accessibility calculations for the four cysteine residues carried out using the crystallographic coordinates (PDB code 1ydv) for both the dimeric and monomeric forms.

The rates of labeling of cysteine residues were monitored using ESI-MS. Fig. 2 shows the electrospray mass spectra of PfTIM taken at different time points after initiating labeling with IAA. Carboxyl methylation leads to a mass increase of 58 Da/modified residue. It is clearly seen that at the end of 4 h, a heterogeneous population of species bearing one, two, three, and four labels is detected. Fig. 3 shows the time course of labeling of cysteine residues in PfTIM using IAA and IAM. To determine the sites of labeling, ESI-MS of peptide fragments generated by trypsin digestion of the unlabeled and differen-

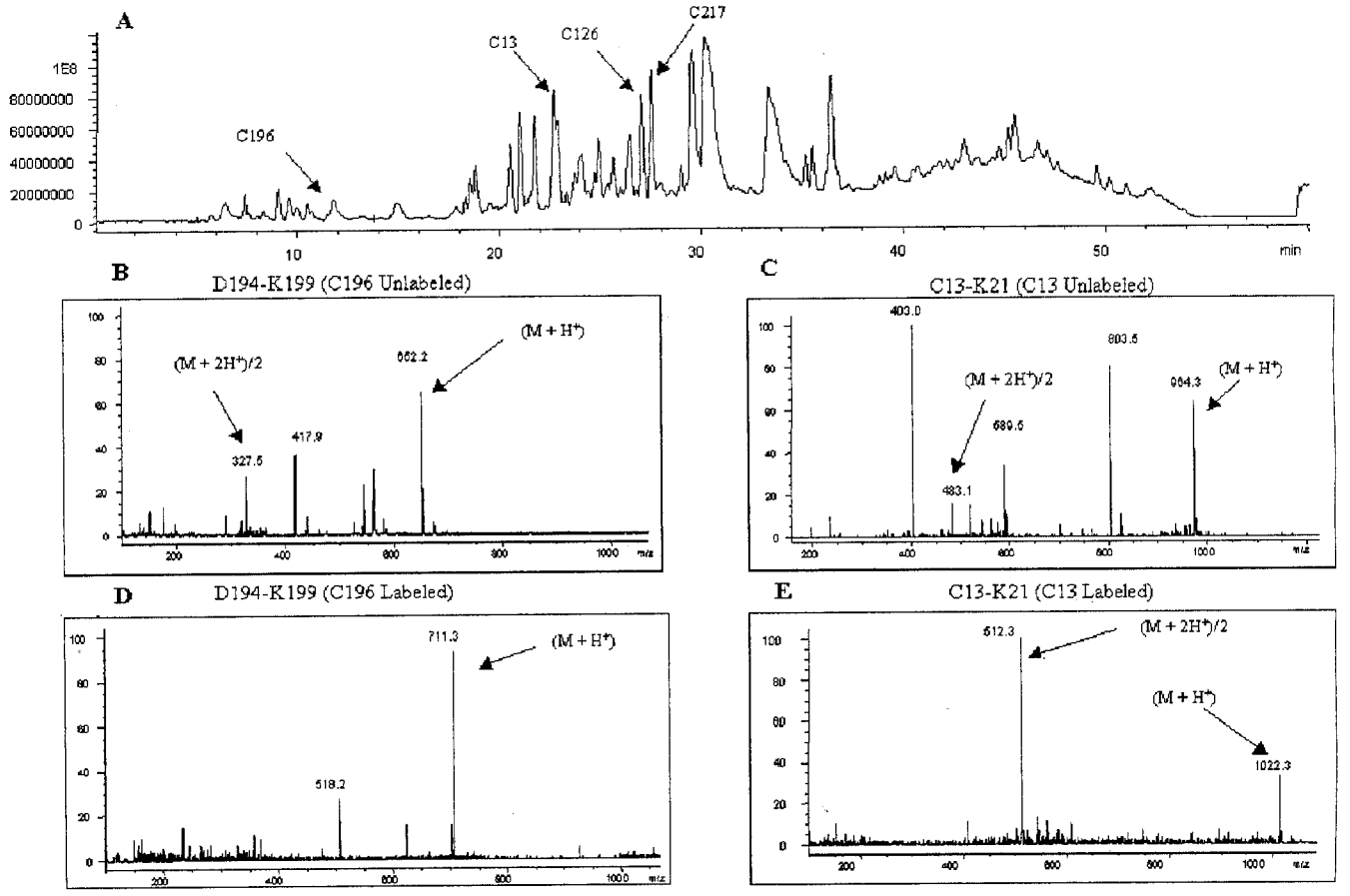


FIG. 4. **Mapping of the IAA-labeled sites using tryptic digests of differentially labeled protein.** *A*, mass-detected reverse phase HPLC profile (total ion chromatogram) of trypsin-digested PfTIM. *B* and *C*, ESI-MS of fragments containing Cys-196 and Cys-13. *D* and *E*, ESI-MS of same fragments after IAA labeling. The error in determining mass is about ±1 Da.

tially labeled protein were compared. Fig. 4 shows a mass detected, reverse phase HPLC profile (total ion chromatogram) of a tryptic digest generated from the wild type enzyme. The peaks corresponding to the peptide fragments bearing the four cysteines are marked. Mass spectra corresponding to representative peaks are shown, and a comparison is made of the spectra obtained after IAA labeling. These studies establish that the rate of cysteine labeling is in the order Cys-196 > Cys-13 ≫ Cys-217/Cys-126. Inspection of the crystal structure confirms that Cys-126 and Cys-217 are almost completely inaccessible to the label in the native conformation. Cys-196 is the most exposed among all cysteine residues present and hence is the most reactive sulfhydryl (Table I). Interestingly, Cys-13, which has only limited accessibility in the native dimeric structure, undergoes fairly rapid modification with both IAA and IAM. During the course of our studies we observed that IAM labeling gradually results in the formation of insoluble protein aggregates, whereas labeling with IAA yielded a soluble protein even after extensive modification. Indeed, rapid labeling of the interface cysteine has also been observed in earlier studies carried out with trypanosomal and leishmanial TIMs (36, 43). This enhanced reactivity may be attributed to cysteine p$K_a$ values, local dynamics at the interface formed by irregular loop structures of the two monomers (loop 3), and occupancy of the catalytic site as suggested by Reyes-Vivas *et al.* (42) for trypanosomal TIM.

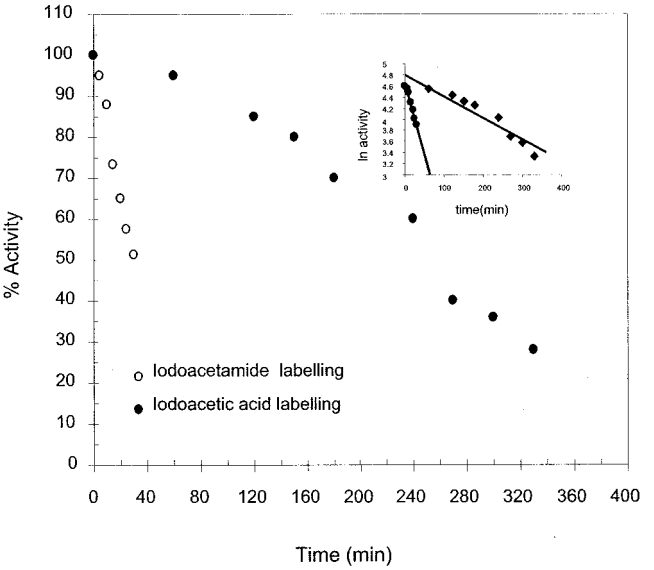


FIG. 5. **Effect of labeling on the enzymatic activity of PfTIM.** The rate of decrease in the enzymatic activity of PfTIM after the initiation of the labeling reaction with IAA and IAM is shown. The *inset* shows the semilog plot of activity (%) *versus* time. The value of the rate constant $k_{obs}$ for the reaction was determined from the slope. The $k_{obs}$ values for IAA and IAM were 0.0039 and 0.0256 $min^{-1}$, respectively.

### *Properties of the Modified Enzyme*

*Enzyme Activity*—Fig. 5 shows the fall in activity as a function of time after the initiation of sulfhydryl labeling with IAA and IAM. In the case of the latter, there is a very rapid fall in the enzymatic activity accompanied by precipitation of the protein. The loss of activity is more gradual in the case of IAA,

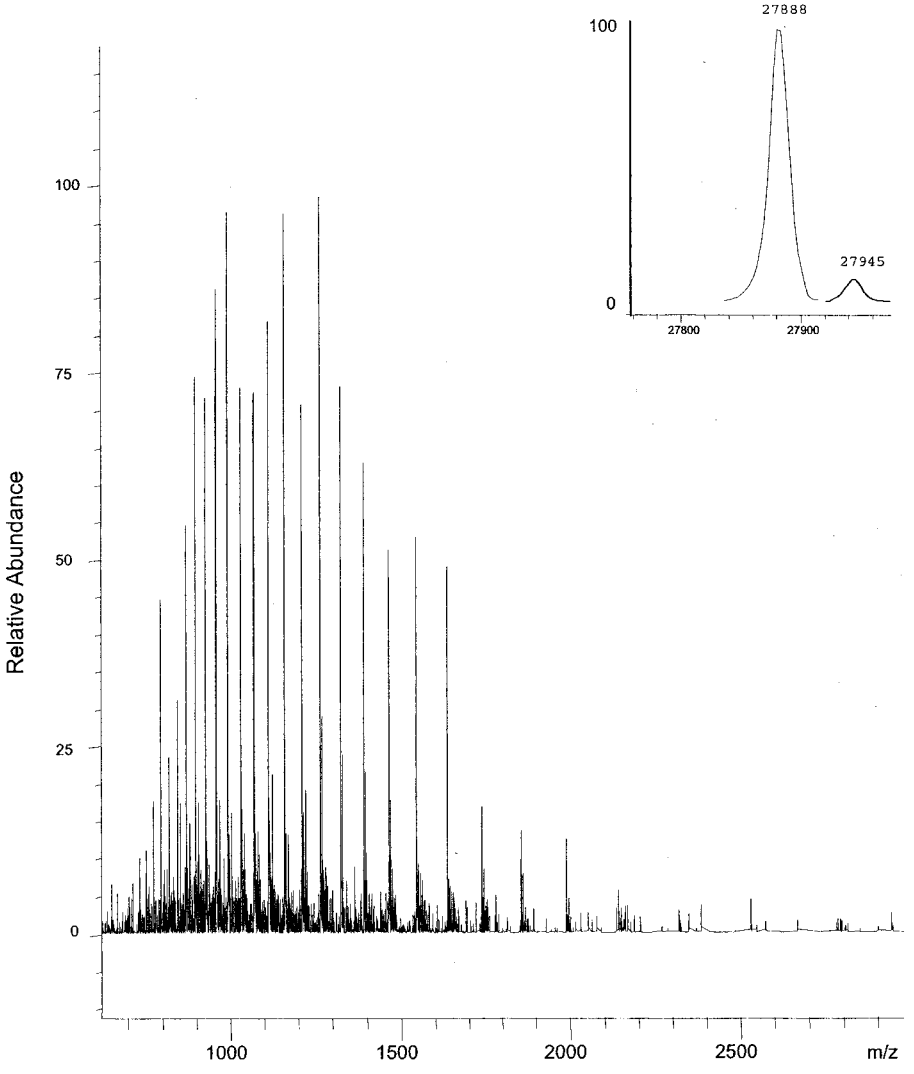


FIG. 6. **IAM-labeled mass spectra of PfTIM.** ESI-MS of singly labeled PfTIM after a 10-min reaction with IAM is shown. The *inset* shows derived masses for the singly labeled species, which is predominant and a relatively small peak for doubly labeled species (~10%).

notably about 30% of the activity is retained even after about 5–6 h of labeling. Because the labeling reagent was in excess, pseudo first-order kinetics was used to calculate the rate constant for the process leading to loss of enzymatic activity. From the slope of the semilog plot (Fig. 5), the rate constants for IAA and IAM were 0.0039 and 0.0256 $min^{-1}$, respectively. Fig. 6 shows the electrospray mass spectra of PfTIM labeled with IAM after 10 min. A singly labeled species (27,888 Da), corresponding to the addition of one carboxamidomethyl group ($\Delta M$ 57 Da) is predominantly observed. A very small amount (approximately 10%) of a doubly labeled species (27,945 Da) is also detected. LC-MS of a tryptic digest at this stage revealed major peptide fragments with the following masses: 8,180, 15,181, and a minor population of 15,238 Da. The species at 8,180 Da corresponds to the fragment Thr-174 to Met-247 (8,123 Da), with the addition of the carboxamidomethyl group. Further tryptic digestion yielded smaller fragments at 710 and 3,386 Da. The former corresponds to the peptide Asp-194 to Lys-199, with an addition of a carboxamidomethyl group, whereas the latter corresponds to Ile-206 to Lys-237 without modification. This suggests that labeling has occurred almost exclusively at Cys-196. The other fragment at 15,181 Da corresponds to the sequence Ala-1 to Arg-133 without modification. This fragment contains both Cys-13 and Cys-126, confirming the absence of modification at these residues. The small population of the 15,238-Da fragment corresponds to the addition of a single carboxamidomethyl group to 15,181 Da (Ala-1 to Arg-133). The smaller peptides obtained from this fragment by further digestion revealed that Cys-13 was labeled, whereas Cys-126 remained unreactive. Therefore from the analysis of the tryptic fragments we infer that the major species is almost exclusively labeled at Cys-196, a conclusion that is supported by the fact that Cys-196 is a surface sulfhydryl, remote from the active site. At this state of labeling the loss of enzyme activity was only 10–12% (Fig. 5). Therefore we conclude that labeling of Cys-196 results in practically no modification of enzymatic activity. On the other hand, Cys-13 is proximate to the active site residue, Lys-12, and is also involved in critical interface contacts (36). The small amount of doubly labeled species in Fig. 6 may then correspond to labeling at both Cys-196 and Cys-13. Correlation of these results with the rates of cysteine labeling suggests that almost all of the loss of the enzymatic activity may be attributed to Cys-13 labeling. A similar loss in enzymatic activity on derivatization of the interface cysteine with the sulfhydryl reagent methyl methanethiosulfonate has been reported for TIMs from *T. brucei*, *T. cruzi*, and *L. mexicana* (12). It is important to note that the presence of some residual activity remaining even after 5 h of labeling can be attributed to presence of unlabeled and/or singly (Cys-196) labeled enzyme, suggesting that the labeling of Cys-196 residue has no appreciable effect on enzymatic activity.

*Size Exclusion Chromatography*—Differentially labeled species of TIMWT were also passed through a calibrated size exclusion gel filtration column to see the effect of labeling on

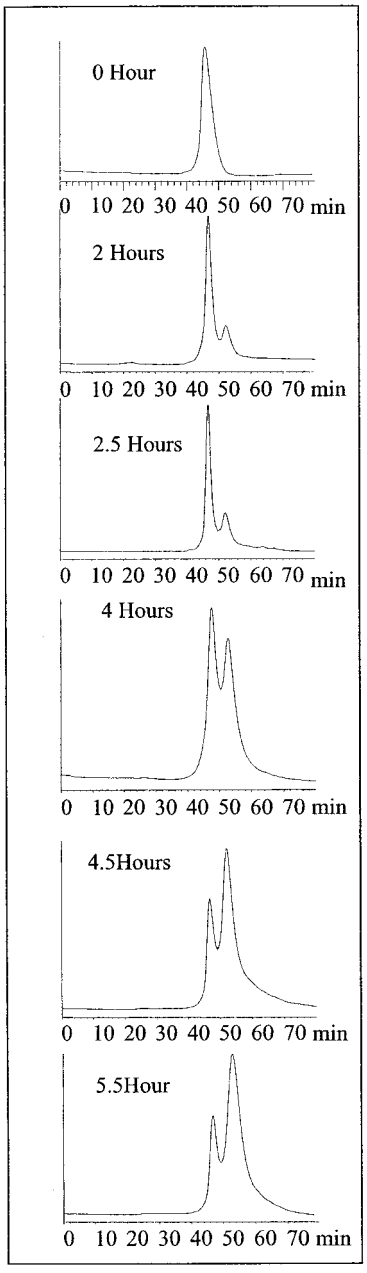


FIG. 7. **Gel filtration elution profiles of IAA-labeled PfTIM.** Gel filtration elution profiles of IAA-labeled TIMWT at different time points are shown. The time after the addition of the reagent is indicated against the *traces*. Note that a comparison of Figs. 5 and 7 reveals a correlation in which an approximately 50% loss in activity is related to the appearance of a second peak at a larger elution volume in the gel filtration profile, with an intensity of about 50% at about 4 h.

the quaternary structure of the protein (Fig. 7). Interestingly, it was observed that after about 2 h of incubation with IAA another peak at a higher elution volume appears, which may be assigned to a monomeric species. Notably, the time course of appearance of the peak ascribed to the monomer (Fig. 7) correlates well with the rate of loss of enzyme activity observed upon labeling (Fig. 5), which in turn has been related to Cys-13 modification by ESI-MS. The appearance of a sharp gel filtration peak at higher elution volumes in the case of the thiol-modified enzyme (Fig. 7) suggests that the monomeric species generated may indeed be substantially folded. Earlier studies on the unfolding of PfTIM with denaturants suggest that an *unfolded* monomer will elute at lower elution volume than the *folded* dimer because of a substantially enhanced hydrodynamic volume in the hydrated state (29). This suggests that as the interface cysteine gets labeled the subunit-subunit interactions are weakened to such an extent that the dimer dissociates.

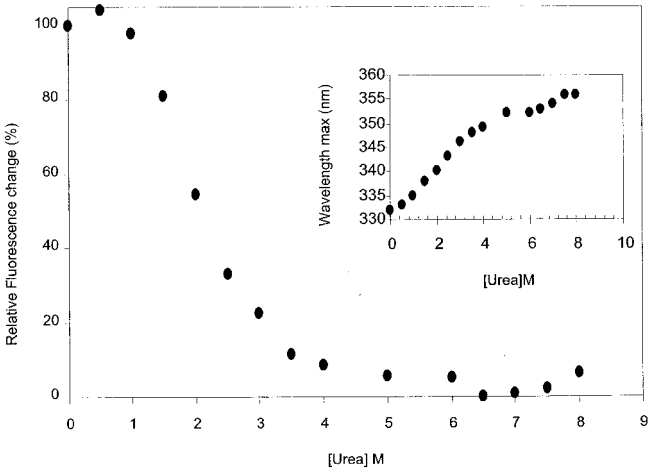


FIG. 8. **Urea denaturation profile of 5-h IAA-labeled PfTIM.** The urea denaturation of TIM species obtained after labeling for 5 h with IAA as monitored by the fluorescence intensity change at 331 nm (excitation at 280 nm) is shown. The *inset* shows the change in emission wavelength with an increasing urea concentration.

An interesting observation in the present study is the dramatically different behavior of the protein when modified with IAA and IAM. In the case of IAA, protein samples remain in solution even after extensive thiol modification. On the contrary, in the case of IAM initial labeling rates are much faster leading to precipitation, observed after 20 min of labeling. Precipitation is undoubtedly a consequence of aggregation of the unfolded form of the modified protein. By correlating the time scales of these observations with the rate of thiol labeling as inferred by mass spectrometry, we conclude that labeling of the interface Cys-13 residue results in subunit dissociation. In the case of IAA the labeled monomer remains substantially folded and soluble, whereas in the case of IAM the labeled monomer probably unfolds, aggregates, and precipitates. IAA labeling results in the introduction of a negative charge at the Cys-13 position; although the reactivity of the charged reagent is lower, the product formed may in fact be structurally stabilized and protected from aggregation by electrostatic effects. Indeed from the available literature on the refolding and unfolding of TIM it is believed that an equilibrium exists between dimer and unfolded monomer, with the folded monomer being an intermediate species (43, 44). A TIM species, generated by labeling for 5 h with IAA in which the predominant form was monomer as evidenced by the gel filtration elution volume profile (Fig. 7) was subjected to urea denaturation (Fig. 8). It was observed that the $C_m$ value (concentration of urea at which 50% of the protein is unfolded) is ~2 M in marked contrast to unlabeled TIM, which shows little evidence for unfolding even until 5 M (see Fig. 10). Here a point to be noted is that the 5-h labeled species is heterogeneous in nature. To probe further the effect of introduction of the negative charge at this critical interface position we created a site-directed mutant, C13D. The aspartic acid and carboxyl methylated cysteine side chains differ only in their chain lengths, with both possessing an ionizable carboxylate group.

### *Properties of the C13D Mutant*

*Characterization of the Purified C13D Mutant Protein*—The mutant protein was obtained by overexpressing the corresponding gene in the *E. coli* strain AA200 (null for TIM) and

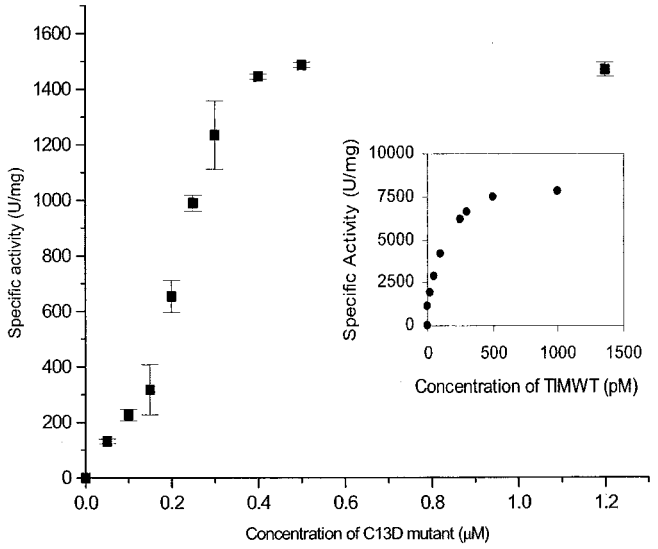


FIG. 9. **Measurement of specific activity of C13D and TIMWT.** The concentration dependence of the enzymatic activity of C13D is shown. The *inset* shows similar concentration dependence in TIMWT.

purifing it using a standard protocol (29, 36). On SDS-PAGE a single band around 28 kDa is seen for C13D. Analysis of C13D by ESI-MS yielded a derived mass of 27,815 Da (expected mass 27,815.5 Da). It should be noted that a mutation A163V has been detected in some clones of wild type PfTIM (36, 29). In the present case the determined mass corresponds to alanine at position 163 and aspartic acid at position 13. The sites of mutations were further identified by mass spectral analysis of tryptic fragments generated from the wild type and the mutant enzyme.

*Enzyme Activity*—Because a critical interface residue has been mutated we considered the possibility of subunit dissociation at concentrations at which enzymatic activity was monitored. The activities of the C13D mutant and the wild type enzyme were therefore determined over a wide range of protein concentrations. Fig. 9 illustrates the concentration dependence of activity in both cases. It is clearly seen that for TIMWT the activity is concentration-independent, above a protein concentration of $0.5 \times 10^{-9}$ M (0.5 nM). At lower concentrations, there is a steep fall in activity. This may be attributed to subunit dissociation and formation of inactive monomers. The C13D mutant shows dramatically different concentration dependence, with a saturating value observed only above a concentration of 0.5 μM. In the region of 0.15–0.3 μM a very steep dependence on concentration is observed. The parameters characterizing the enzymatic activity ($k_{cat}$ and $K_m$) were determined for the two proteins in a regime where no concentration dependence of activity is observed. Under these conditions, the mutant protein was found to have a specific activity of 1,250–1,500 units/mg of protein. In contrast, the wild type enzyme had a specific activity of 7,800–8,000 units/mg of protein, suggesting that the mutation has led to an appreciable decrease in the enzymatic activity. Table II summarizes the kinetic parameters of the wild type and the mutant enzymes. It is observed that the $K_m$ values for the mutant and the wild type are very similar, but the $k_{cat}$ for the C13D mutant is almost ~7-fold lower. This loss of activity in the mutant may be a consequence of local structural adjustments in the vicinity of the mutation. It is pertinent that Lys-12, a critical active site residue that adopts an unusual positive value for the dihedral angle $\phi$ in all known native TIM crystal structures (36, 45), is adjacent to the site of mutation.

*Gel Filtration*—Gel filtration studies with C13D reveal that with lowering of the protein concentration there was a steady increase in the elution volume (data not shown). The observed gel filtration profiles showed only a single, sharp and symmetrical peak suggesting that the time scale of equilibration between the monomeric and dimeric species is fast, precluding resolution of the two distinct states. This may be contrasted with the behavior observed for chemically modified protein, where dissociation follows carboxyl methylation at Cys-13 (Fig. 7). Distinct peaks corresponding to both dimeric and monomeric species have been observed earlier for the subunit interface mutant Y74G. The origin of widely differing rates of monomer-dimer equilibration is not clear at present.

TABLE II
*Kinetic properties of TIMWT and the mutant C13D*

| | Specific activity | $K_m$ | $k_{cat}$ |
|---|---|---|---|
| | *units/mg* | *mM* | $\times 10^5\ min^{-1}$ |
| TIMWT | 7,800–8,000 | 0.35 ± 0.16 | 2.68 ± 0.84 |
| C13D | 1,250–1,500 | 0.31 ± 0.08 | 0.36 ± 0.07 |

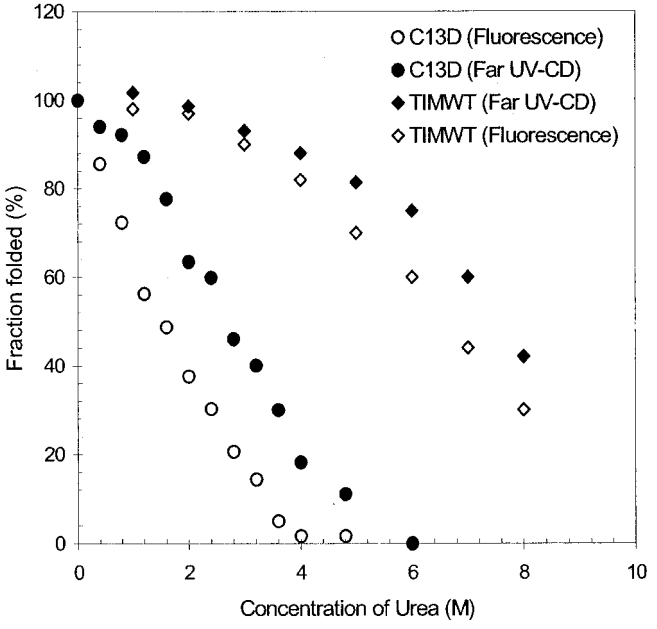


FIG. 10. **Comparison of the stability of C13D mutant and wild type PfTIM.** Effect of urea on TIMWT and C13D mutant monitored by protein fluorescence ($\lambda_{em}$ = 331 nm) and far UV-CD studies ($[\theta]_{220\ nm}$).

*Stability of C13D Mutant*—The stability of the wild type and the mutant to denaturants was compared using various spectroscopic methods. Equilibrium denaturation studies in urea showed that TIMWT retains considerable structure even in 8 M urea (29). It is seen that until 6 M urea there is no significant change in the emission maximum ($\lambda_{em}$), and the emission intensity drops by only 30–40%. However, there is a sharp change between 6 and 8 M urea in the emission intensity, suggesting a significant change in the Trp environment (Fig. 10). In the case of the C13D mutant we obtained the $C_m$ value of 1.6 M, which indicated a dramatic lowering of stability to urea denaturation. The changes in the secondary structure of the two proteins with urea were monitored using far UV-CD measurements at 220 nm. It is again observed that although TIMWT does not show any substantial loss in the secondary structure even at 8 M urea, the secondary structure of the mutant collapses by a urea concentration of 4 M (Fig. 10). Similar observations were made when guanidinium chloride was used as a denaturant. In this case, TIMWT had a $C_m$ of 1.2 M, whereas C13D had a low $C_m$ of 0.6 M (data not shown).

## CONCLUSION

The present study demonstrates that chemical modification of a reactive cysteine residue at the subunit interface of PfTIM can lead to large structural perturbations and concomitant loss of enzymatic activity. Dissection of the differential reactivity of the four cysteine residues in PfTIM permits us to conclude that the loss of enzymatic activity correlates well with labeling of the interface cysteine Cys-13. This observation assumes significance in view of the absence of a reactive thiol at the corresponding site in the human enzyme. Carboxyl methylation at Cys-13 constitutes a major perturbation leading to subunit dissociation. Studies with the site-directed mutant C13D suggest that introduction of the negative charge at the interface is indeed destabilizing. However, a substantially smaller size of the Asp residue compared with carboxyl methyl cysteine allows the former to maintain a dimeric structure, albeit less stable than the wild type. Thus, targeted chemical modification of parasitic enzymes, which exploits structural differences with the host enzyme, may prove useful in approaches to inhibit them.

*Acknowledgments*—We thank Ali Asgar Yunus for help during the initial experiments, Nijaguna Prasad for initial work in generating the C13D mutant, and S. Kumar Singh for assistance in making Fig. 1.

## REFERENCES

1. Suresh, S., Turley, S., Opperdoes, F. R., Michels, P. A., and Hol, W. G. J. (2000) *Structure Fold. Des.* **8,** 541–552
2. Subbayya, I. N., Ray, S. S., Balaram, P., and Balaram, H. (1997) *Indian J. Med. Res.* **106,** 79–94
3. Phillips, C., Dohnalek, J., Gover, S., Barrett, M. P., and Adams, M. J. (1998) *J. Mol. Biol.* **282,** 667–681
4. Somoza, J. R., Skillman, A. G., Jr., Munagala, N. R., Oshiro, C. M., Knegtel, R. M., Mpoke, S., Fletterick, R. J., Kuntz, I. D., and Wang, C. C. (1998) *Biochemistry* **37,** 5344–5348
5. Luecke, H., Prosise, G. L., and Whitby, F. G. (1997) *Exp. Parasitol.* **87,** 203–211
6. Li, C. M., Tyler, P. C., Furneaux, R. H., Kicska, G., Xu, Y., Grubmeyer, C., Girvin, M. E., and Schramm, V. L. (1999) *Nat. Struct. Biol.* **6,** 582–587
7. Fairlamb, A. H., and Cerami, A. (1992) *Annu. Rev. Microbiol.* **46,** 695–729
8. Verlinde, C. L. M. J., Merritt, E. A., Van Den Akker, F., Ki, H., Feil, I., Delboni, L. F., Mande, S. C., Sarfaty, S., Petra, P. H., and Hol, W. G. J. (1994) *Protein Sci.* **3,** 1670–1686
9. Babe, L. M., Rose, J., and Craik, C. S. (1992) *Protein Sci.* **1,** 1244–1253
10. Shoichet, B. K., Stroud, R. M., Santi, D. V., Kuntz, I. D., and Perry, K. M. (1993) *Science* **259,** 1445–1450
11. Kuntz, D. A., Osowski, R., Schudok, M., Wierenga, R. K., Muller, K., Kessler, H., and Opperdoes, F. R. (1992) *Eur. J. Biochem.* **207,** 441–447
12. Gomez-Puyou, A., Saavedra-Lira, E., Becker, I., Zubillaga, R. A., Rojo-Dominguez, A., and Perez-Montfort, R. (1995) *Chem. Biol.* **2,** 847–855
13. Smith, D. J., Maggio, E. T., and Kenyon, G. L. (1975) *Biochemistry* **4,** 766–771
14. Welches, W. R., and Baldwin, T. O. (1981) *Biochemistry* **20,** 512–517
15. Garza-Ramos, G., Perez-Montfort, R., Rojo-Dominguez, A., de Gomez-Puyou, M. T., and Gomez-Puyou, A. (1996) *Eur. J. Biochem.* **241,** 114–120
16. Opperdoes, F. R. (1987) *Annu. Rev. Microbiol.* **41,** 127–151
17. Opperdoes, F. R., and Borst, P. (1997) *FEBS Lett.* **80,** 360–364
18. Willson, M., Lauth, N., Perie, J., Callens, M., and Opperdoes, F. R. (1994) *Biochemistry* **33,** 214–220
19. Knowles, J. R. (1991) *Nature* **350,** 121–124
20. Lambeir, A. M., Opperdoes, F. R., and Wierenga, R. K. (1987) *Eur. J. Bochem.* **168,** 69–74
21. Maes, D., Zeelen, J. P., Thanki, N., Beaucamp, N., Alvarez, M., Thi, M. H., Backmann, J., Martial, J. A., Wyns, L., Jaenicke, R., and Wierenga, R. K. (1999) *Proteins* **37,** 441–453
22. Walden, H., Bell, G. S., Russell, R. J., Siebers, B., Hensel, R., and Taylor, G. L. (2001) *J. Mol. Biol.* **306,** 745–757
23. Hol, W. G. J., Vellieux, F. M. D., Verlinde, C. M. J., Wierenga, R. K., Noble, M. E. M., and Read, R. J. (1991) in *Molecular Conformation and Biological Interactions* (Balaram, P., and Ramaseshan, S., eds) pp. 215–244, Indian Academy of Sciences, Bangalore, India
24. Waley, S. G. (1973) *Biochem. J.* **135,** 165–192
25. Schliebs, W., Thanki, N., Jaenicke, R., and Wierenga, R. K. (1997) *Biochemistry* **36,** 9655–9662
26. Borchert, T. V., Zeelen, J. P., Schliebs, W., Callens, M., Minke, W., Jaenicke, R., and Wierenga, R. K. (1995) *FEBS Lett.* **367,** 315–318
27. Mainfroid, V., Terpstra, P., Beauregard, M., Frere, J. M., Mande, S. C., Hol, W. G., Martial, J. A., and Goraj, K. (1996) *J. Mol. Biol.* **257,** 441–456
28. Lambeir, A. M., Backmann, J., Ruiz-Sanz, J., Filimonov, V., Nielsen, J. E., Kursula, I., Norledge, B. V., and Wierenga, R. K. (2000) *Eur. J. Biochem.* **267,** 2516–2524
29. Gokhale, R. S., Ray, S. S., Balaram, H., and Balaram, P. (1999) *Biochemistry* **38,** 423–431
30. Gopal, B., Ray, S. S., Gokhale, R. S., Balaram, H., Murthy, M. R. N., and Balaram, P. (1999) *Biochemistry* **38,** 478–486
31. Sampson, N. S., and Knowles, J. R. (1992) *Biochemistry* **31,** 8482–8487
32. Lodi, P. J., Chang, L. C., Knowles, J. R., and Komives, E. A. (1994) *Biochemistry* **33,** 2809–2814
33. Casal, J. I., Ahern, T. J., Davenport, R. C., Petsko, G. A., and Klibanov, A. M. (1987) *Biochemistry* **26,** 1258–1264
34. Wierenga, R. K., Noble, M. E., Vriend, G., Nauche, S., and Hol, W. G. J. (1991) *J. Mol. Biol.* **220,** 995–1015
35. Maldonado, E., Soriano-Garcia, M., Moreno, A., Cabrera, N., Garza-Ramos, G., de Gomez-Puyou, M., Gomez-Puyou, A., and Perez-Montfort, R. (1998) *J. Mol. Biol.* **283,** 193–203
36. Velanker, S. S., Ray, S. S., Gokhale, R. S., Suma, S., Balaram, H., Balaram, P., and Murthy, M. R. N. (1997) *Structure* **5,** 751–761
37. Kohl, L., Callens, M., Wierenga, R. K., Opperdoes, F. R., and Michels, P. A. (1994) *Eur. J. Biochem.* **220,** 331–338
38. Garza-Ramos, G., Cabrera, N., Saavedra-Lira, E., de Gomez-Puyou, M. T., Ostoa-Saloma, P., Perez-Montfort, R., and Gomez-Puyou, A. (1998) *Eur. J. Biochem.* **253,** 684–691
39. Perez-Montfort, R., Garza-Ramos, G., Alcantara, G. H., Reyes-Vivas, H., Gao, X. G., Maldonado, E., de Gomez-Puyou, M. T., and Gomez-Puyou, A. (1999) *Biochemistry* **38,** 4114–4120
40. Ranie, J., Kumar, V. P., and Balaram, H. (1993) *Mol. Biochem. Parasitol.* **61,** 159–169
41. Plaut, B., and Knowles, J. R. (1972) *Biochem. J.* **129,** 311–320
42. Reyes-Vivas, H., Hernandez-Alcantara, G., Lopez-Velazquez, G., Cabrera, N., Perez-Montfort, R., Tuena de Gomez-Puyou, M., and Gomez-Puyou, A. (2001) *Biochemistry* **40,** 3134–3140
43. Rietveld, A. W., and Ferreira, S. T. (1998) *Biochemistry* **37,** 933–937
44. Zabori, S., Rudolph, R., and Jaenicke, R. (1980) *Z. Naturforsch.* **35,** 999–1004
45. Wierenga, R. K., Noble, M. E., and Davenport, R. C. (1992) *J. Mol. Biol.* **224,** 115–126
46. Chothia, C. (1976) *J. Mol. Biol.* **105,** 1–12